

## Equator-S observations of He<sup>+</sup> energization by EMIC waves in the dawnside equatorial magnetosphere

C. G. Mouikis,<sup>1</sup> L. M. Kistler,<sup>1</sup> W. Baumjohann,<sup>2</sup> E. J. Lund,<sup>1</sup> A. Korth,<sup>3</sup>  
B. Klecker,<sup>4</sup> E. Möbius,<sup>1</sup> M. A. Popecki,<sup>1</sup> J. A. Sauvaud,<sup>5</sup> H. Rème,<sup>5</sup>  
A. M. Di Lellis,<sup>6</sup> M. McCarthy,<sup>7</sup> and C. W. Carlson<sup>8</sup>

Received 7 August 2001; revised 15 February 2002; accepted 19 February 2002; published 25 May 2002.

[1] We present Equator-S observations of He<sup>+</sup> energization by electromagnetic ion cyclotron (EMIC) waves in the dawn side equatorial magnetosphere at  $L > 7$ . The He<sup>+</sup> ions are transversely accelerated up to 2 keV, which is almost an order of magnitude higher than found in previous observations. The heating signatures are correlated, on short time scales (in the order of a few minutes or less), with the presence of EMIC wave emissions in the vicinity of the He<sup>+</sup> gyrofrequency (Pc1 frequency range). These events were observed during quiet magnetospheric conditions at the inner edge of the plasmasheet. At this boundary 10 to 40 keV protons, which convect on open drift paths, exhibit a pronounced pitch angle anisotropy providing the free energy for the enhancement of the Pc1 emissions. **INDEX TERMS:** 2772 Magnetospheric Physics: Plasma waves and instabilities; 7867 Space Plasma Physics: Wave/particle interactions; 2768 Magnetospheric Physics: Plasmasphere

### 1. Introduction

[2] Observations suggesting He<sup>+</sup> energization by electromagnetic ion cyclotron (EMIC) waves in the magnetosphere have been reported previously [Mauk *et al.*, 1981; Young *et al.*, 1981; Anderson and Fuselier, 1994; Fuselier and Anderson, 1996]. The EMIC waves can be generated in the equatorial magnetosphere from the ion cyclotron instability driven by anisotropic ( $T_{\perp p} > T_{\parallel p}$ ) energetic (10 keV to 50 keV) proton populations [Cornwall, 1965; Kennel and Petschek, 1966]. In the presence of low energy He<sup>+</sup>, these waves will interact resonantly with He<sup>+</sup>, heating it perpendicular to the magnetic field direction [Gendrin and Roux, 1980]. Mauk *et al.* [1981] using data from the ATS-6 geostationary satellite, reported events where cyclotron phase bunched helium ions (20–200 eV) were observed in the vicinity of EMIC waves. Young *et al.* [1981] using GEOS-1 and GEOS-2 data, reported events near geostationary orbit, where the He<sup>+</sup> ions were energized up to a few hundred eV after the onset of EMIC waves. They reported that the He<sup>+</sup> flux below 110 eV became anisotropic in a direction mainly perpendicular to the magnetic field. Roux *et al.* [1982], using the same data set, found that the He<sup>+</sup> flux was modulated at the EMIC wave frequency suggesting that the He<sup>+</sup> ions are trapped in the potential troughs of the wave. They concluded that nonlinear trapping is responsible for the acceleration of He<sup>+</sup>. Anderson and Fuselier [1994] and Fuselier and

Anderson [1996], using composition data from AMPTE/CCE, reported a correlation between periods of EMIC wave activity and anisotropic ( $T_{\perp \text{He}^+} > T_{\parallel \text{He}^+}$ ) He<sup>+</sup> distributions with energies from  $\approx 1$  to 160 eV. These events were detected in the dawn to noon side of the magnetosphere and beyond  $L \approx 7$ .

[3] Anderson *et al.* [1992a] studied the occurrence distribution of EMIC waves in the equatorial magnetosphere. They identified two regions, the early afternoon region ( $L > 7$ , MLT = 1100 to 1500) and the dawn region ( $L > 7$ , MLT = 0300 to 0900), where there is a high occurrence rate of EMIC waves. They suggested that the predominance of  $L > 7$  events implies that plasma sheet ion distributions develop sufficient temperature anisotropy to generate EMIC waves on a routine basis in their drift from the nightside to the dayside and that the plasma sheet ions on open drift paths may present the greatest energy source for equatorially generated EMIC waves. In addition they studied the wave properties of these events [Anderson *et al.*, 1992b] where they found that EMIC waves at dawn (in the region 0300–0900 MLT) have linear rather than left-hand polarization and have higher normalized frequencies  $X$  ( $X = f/f_{\text{H}^+}$  where  $f$  and  $f_{\text{H}^+}$  are the wave frequency and the proton gyrofrequency, respectively) than noon-time events. Anderson *et al.* [1996] proposed that these active dawn events are driven by protons that have convected by the dawnside and are therefore relatively fresh solar wind ions.

[4] In this letter we present new observational evidence of He<sup>+</sup> energization by EMIC waves in the dawnside equatorial magnetosphere. These observations show transverse He<sup>+</sup> energization up to 2 keV which is almost an order of magnitude higher than previous observations. These events were observed during quiet magnetospheric conditions at the inner edge of the plasmasheet, at  $L > 7$ , where protons in the energy range 10 to 40 keV exhibited a pronounced pitch angle anisotropy.

### 2. Mission and Instrumentation

[5] Equator-S was in a highly elliptical orbit with an apogee of 11  $R_E$  and a perigee of 500 km. It orbited in the geographic equatorial plane (inclination 3.9°). The initial apogee was at 1100 MLT, and it then precessed toward earlier local times. Data shown here are from the Equator-S Ion Composition instrument (ESIC) and the magnetic field instrument (MAM). ESIC measured the 3-dimensional distribution functions of the major species (H<sup>+</sup>, O<sup>+</sup>, He<sup>++</sup>, He<sup>+</sup>) in the magnetosphere and magnetosheath over the energy range 20 eV/e – 40 keV/e. It is a combination of a top-hat electrostatic analyzer followed by post-acceleration of 15–18 keV, and then a time-of-flight measurement, similar to the CIS1 instrument designed for CLUSTER [Rème *et al.*, 1997] and the TEAMS instrument on FAST [Möbius *et al.*, 1998]. Full velocity distributions are obtained every 1.5 seconds (spin period) in the high-rate mode of data acquisition and every 6 seconds in the low-rate mode. The magnetic field instrument [Fornacon *et al.*, 1999] consisted of two three-axis flux-gate magnetometers with a sampling rate of 128 vectors/s when only one of the magnetometers was utilized, and 64 vectors/s when both were utilized. This sampling frequency

<sup>1</sup>University of New Hampshire, Durham, USA.

<sup>2</sup>Institut für Weltraumforschung, Graz, Austria.

<sup>3</sup>Max-Planck-Institut für Aeronomie, Lindau, Germany.

<sup>4</sup>Max-Planck-Institut für extraterrestrische Physik, Garching, Germany.

<sup>5</sup>C.E.S.R., Toulouse, France.

<sup>6</sup>I.F.S.I., Rome, Italy.

<sup>7</sup>University of Washington, Seattle, WA, USA.

<sup>8</sup>University of California, Berkeley, CA, USA.

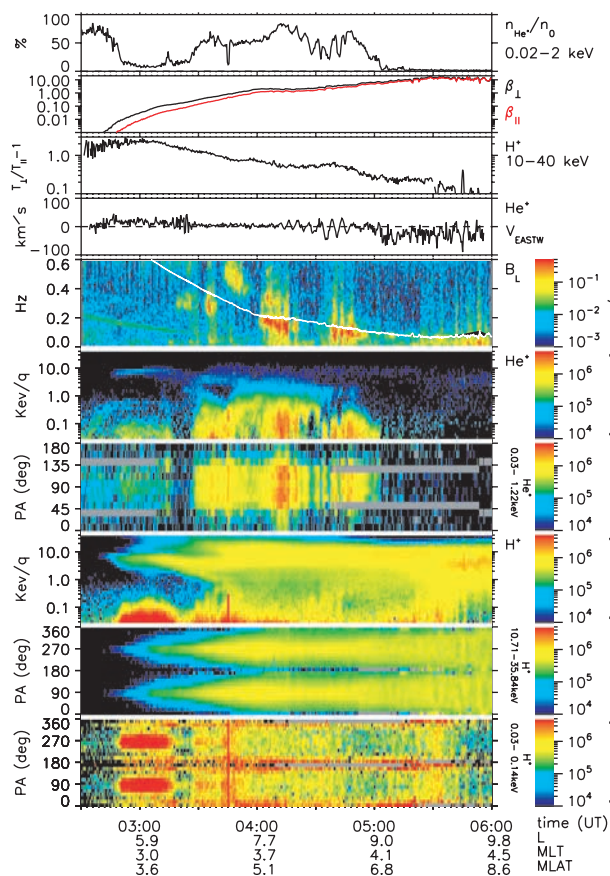


**Figure 1.** An overview of particle and magnetic field data from the March 10th, 1998, outbound pass. From top to bottom, the panels show the relative He<sup>+</sup> concentration for ions with energy 0.02 to 2 keV; the perpendicular ( $\beta_{\perp}$ ) and parallel ( $\beta_{\parallel}$ ) plasma beta; the temperature anisotropy of protons with energy 10 to 40 keV; the eastward component of the He<sup>+</sup> bulk velocity; the dynamic spectrum of the left hand polarized transverse magnetic field component (the white line indicates the local He<sup>+</sup> gyrofrequency); the He<sup>+</sup> energy spectra; the low energy He<sup>+</sup> pitch angle distribution; the H<sup>+</sup> energy spectra; the high energy proton pitch angle distribution; and the low energy proton pitch angle distribution.

is adequate for the study of the EMIC emissions which in the magnetosphere don't exceed a few Hz.

### 3. Observations

[6] Figure 1 displays an overview of particle and magnetic field data from the March 10th, 1998, outbound pass. Local time of apogee was at  $\sim$ 0600 MLT. From top to bottom, the panels show the relative He<sup>+</sup> concentration,  $n_{\text{He}^+}/n_0$  ( $n_0$  is the total ion density), for ions with energy 0.02 to 2 keV; the perpendicular ( $\beta_{\perp}$ ) and parallel ( $\beta_{\parallel}$ ) plasma beta; the temperature anisotropy  $A_p = T_{\perp p}/T_{\parallel p} - 1$ , where  $T_{\perp p}$  and  $T_{\parallel p}$  are the perpendicular and parallel temperatures, respectively, of protons with energy 10 to 40 keV; the eastward (azimuthal) component of the He<sup>+</sup> bulk velocity; the dynamic spectrum of the left hand polarized transverse magnetic field component over the frequency range 0.01–0.6 Hz (the white line indicates the local He<sup>+</sup> gyrofrequency); the He<sup>+</sup> energy spectra (differential number flux); the He<sup>+</sup> low energy, 0.03 keV–1.22 keV, pitch angle spectra; the H<sup>+</sup> energy spectra; the H<sup>+</sup> high energy,

10.71 keV–35.84 keV, pitch angle spectra; and the H<sup>+</sup> low energy, 0.03 keV–0.14 keV, pitch angle spectra.

[7] At  $\sim$ 0300 UT Equator-S had exited the plasmopause and was in the plasmashet. From electric field and plasma density observations of the POLAR/EFI experiment the plasmopause position was estimated to be at  $L \sim 5.8$  (H. Laakso, private communication, 2000). During the next  $\sim$ 2 hours, from 0325 to 0505 UT, Equator-S encountered a region where He<sup>+</sup> heating up to  $\sim$ 2 keV was observed (Figure 1, 6th panel). During this time interval the satellite was in the pre-dawn region (0300–0400 MLT), fairly close to the magnetic equator ( $4^{\circ}$ – $7^{\circ}$  MLAT) and moved outwards from  $L = 6.5$  to  $L = 9.0$ . The plasma  $\beta$  ranged from 0.1 to 1 (Figure 1, 2nd panel). The He<sup>+</sup> heating is not continuous. There are three distinct intervals (0327–0350 UT, 0400–0420 UT, 0438–0451 UT), where He<sup>+</sup> is heated, from which the later two show a substructure with a period of  $\sim$ 5 min. This modulation of the particle fluxes can be clearly seen in the azimuthal component of the He<sup>+</sup> bulk velocity (Figure 1, 4th panel) indicating the presence of a fundamental mode toroidal Pc 5. The He<sup>+</sup> low energy pitch angle distribution shows that this population is perpendicularly accelerated (Figure 1, 7th panel).

[8] These He<sup>+</sup> heating intervals are associated with the presence of wave emissions below and above the He<sup>+</sup> gyrofrequency (Pc 1 frequency range), as seen in the magnetic field dynamic spectrum (Figure 1, 5th panel). There is a close correlation between these emissions and the intensification of the He<sup>+</sup> fluxes. Intervals where no emissions are present correspond to intervals where He<sup>+</sup> heating ceases. In addition they show the same Pc 5-type ( $\sim$ 5 min period) modulation (during the last two heating intervals). The emissions below  $f_{\text{He}^+}$  exhibit left hand polarization while the emissions above  $f_{\text{He}^+}$  exhibit left hand or linear polarization. The wave emissions stop when the proton temperature anisotropy  $A_p$  (Figure 1, 3rd panel) becomes smaller than  $\sim$ 0.25.

[9] The close correlation (in the order of a few minutes or less) between the He<sup>+</sup> acceleration and the EMIC waves are suggestive of a cyclotron resonant acceleration mechanism which in a single-stage process can preferentially accelerate cold He<sup>+</sup> ions to energies up to 2 keV. Although the ESIC instrument does not measure the cold populations, we have the following indirect evidence that the initial energy of the He<sup>+</sup> ions was below 20 eV (the low energy threshold of ESIC). The relative He<sup>+</sup> concentration observed by ESIC (Figure 1, top panel) during the heating interval is  $\eta = n_{\text{He}^+}/n_0 \approx 80\%$ . This is a highly overestimated value and is an artifact of the preferential heating of He<sup>+</sup> which brings more He<sup>+</sup> in the energy window of the instrument [Anderson and Fuselier, 1994] Alternatively, an estimation of the relative He<sup>+</sup> concentration can be obtained using the observed cutoff,  $X_{co} = (1 +$

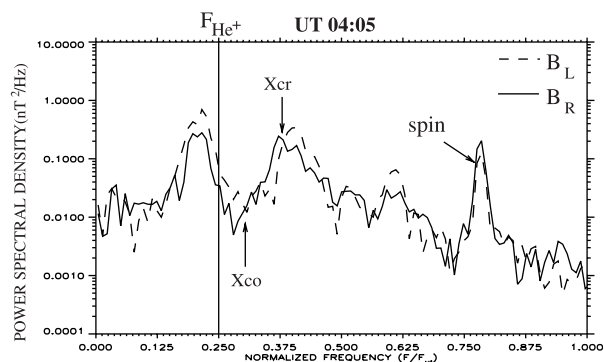


**Figure 2.** Power spectral density over normalized frequency  $X = f/f_{\text{He}^+}$ . The dashed (solid) line shows the left (right) handed spectral power.

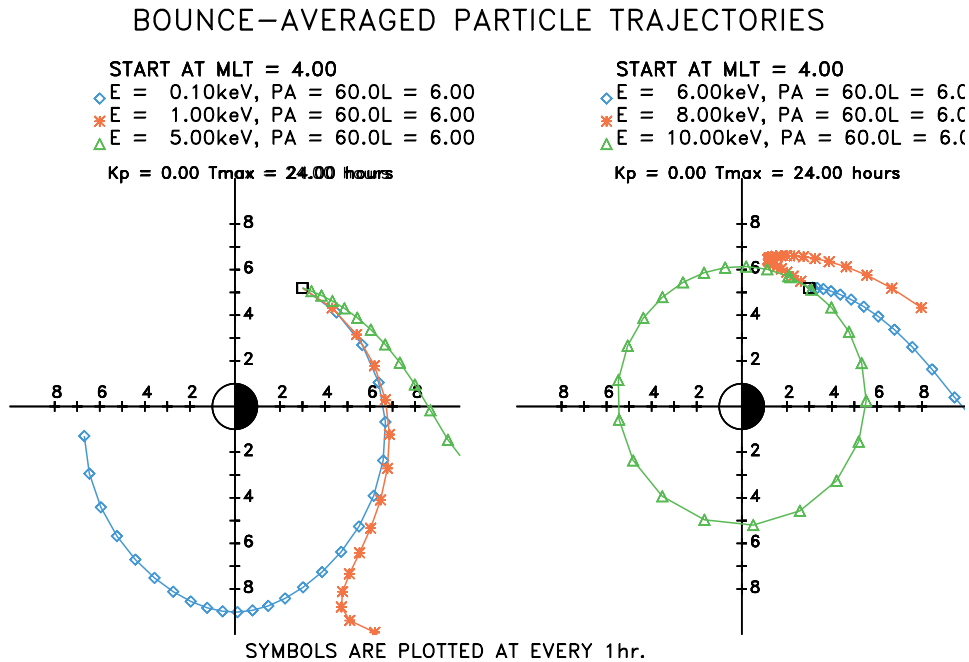


**Figure 3.** Drift paths for ions observed at  $L = 6.0$ , 0400 MLT, at 6 representative energies, 0.1, 1, 5, 6, 8, and 10 keV/e.

$3\eta/4$ , and cross over,  $X_{cr} = (1 + 15\eta)^{1/2}/4$ , frequencies [Gendrin and Roux, 1980]. Figure 2 shows an example of the magnetic field power spectrum versus the normalized frequency  $X$  that corresponds to a He<sup>+</sup> energization event. The dashed (solid) line shows the left (right) handed spectral power density. The formation of a stop band above the  $f_{He^+}$ , due to the presence of He<sup>+</sup> in the ambient plasma [Gendrin and Roux, 1980], introduces a cutoff frequency at  $X_{co} = 0.31$  while the cross over frequency is at  $X_{cr} = 0.375$ . Both these values give an estimated relative concentration value  $\eta = 8\%$  in agreement with Mauk *et al.* [1981]. Thus, the apparent high values of relative He<sup>+</sup> concentration, as observed by ESIC, are due to the preferential heating of He<sup>+</sup> which increases the proportion of He<sup>+</sup> detected by the instrument.

[10] The He<sup>+</sup> heating is observed at the inner edge of the plasma sheet, where high energy (10–20 keV) ions can penetrate to lower L-shells than the low energy (<1 keV) ions. Ejiri *et al.* [1980] modeled the time dependence of the inner penetration distance as a function of energy, and showed that for the energetic particles to drift in significantly further than the low energy ions, drift times greater than 9 hours are required. This feature is observed at two locations during this pass, at  $\sim 0340$  UT ( $L \sim 7.0$ ) and  $\sim 0525$  UT ( $L \sim 9.5$ ). In both cases the flux of the 0.1–1 keV population drops off with decreasing  $L$ , while the high energy particles extend further in. That this feature is observed in two locations is most likely an indication that there is time dependence in the electric field which defines this boundary. First the boundary developed at the lower  $L$ -values. Then the electric field weakened, and the boundary moved out to higher  $L$ -values. However, because of the slow drift speeds of the ions, the inner boundary is still visible in the particle signatures. Inside this region protons with energies between 10 and 40 keV are strongly anisotropic (Figure 1, 2nd panel from bottom) while they become isotropic at higher  $L$  shells. This anisotropy is better shown in the proton temperature anisotropy plot (Figure 1, 3rd panel). The temperature anisotropy,  $A_p$ , ranges from values greater than 1 at small  $L$ -shells ( $L \sim 6-7$ ) down to  $\sim 0.1$  at the end of the inner edge of the plasma sheet. This region is also characterized by the presence of low energy (up to  $\sim 100$  eV) field aligned proton populations (Figure 1, bottom panel), which

are usually observed in this region and are of ionospheric origin [Nagai *et al.*, 1983].

#### 4. Discussion

[11] Several other events of preferential perpendicular acceleration of cold He<sup>+</sup> ions to energies up to  $\sim 2$  keV have been identified in the Equator-S data set. All events were observed during fairly quiet magnetospheric conditions at the inner edge of the plasma sheet. This region should not be viewed as a spatial region, but as a temporal state in the evolution of the convecting plasma sheet populations which during relatively quiet magnetospheric conditions can be at high  $L$  shells ( $L \simeq 9-12$ ). The proton anisotropy which develops in this region can provide the free energy for the generation of the instability. The proton temperature anisotropy ( $A_p = T_{\perp p}/T_{\parallel p} - 1$ ) develops because the drift to this region is slow enough that charge exchange has a significant effect. We have modeled this phenomenon using a dipole magnetic field combined with a Volland-Stern electric field. Figure 3 shows the drift trajectories for ions that arrive at  $L = 6$  and 0400 MLT at 6 different energies. Note that the 8 keV drift path has taken 14 hours to drift to this location. Thus, at this boundary, the drifts are slow enough to give the observed anisotropy.

[12] Another characteristic of the inner edge of the plasmasheet region is the presence of low energy ( $\sim 100$  eV) field aligned protons. These field aligned protons are always present during the He<sup>+</sup> energization periods and their cessation usually coincides with the end of the He<sup>+</sup> energization events, indicating that the low energy field aligned protons might be contributing to the instability.

[13] In addition, for the event presented here, toroidal Pc 5 pulsations modified periodically the background plasma parameters causing onsets and cessations of the Pc 1 emissions. The Pc 5 pulsations could be related to the presence of a fairly abrupt increase in the solar wind density during this event. Toroidal Pc 5 resonances are a common occurrence in the dawn flank of the magnetosphere for  $L > 8$  [Anderson *et al.*, 1990] and close to the equator they can be best seen in the electric field or plasma velocity data (azimuthal direction). Such modulation of Pc 1 emissions by



Pc 5 pulsations, which is a common occurrence in the Equator-S data set, can alter the polarization of the EMIC waves off the equator introducing propagation effects analogous to the propagation effects presented by [Rauch and Roux, 1982]. This could explain the Anderson et al. [1992b] observations that in the dawn region the polarization of the EMIC waves is linear instead of left handed.

[14] From the study of this event in which He<sup>+</sup> is accelerated to 2 keV, we have determined that:

1. EMIC waves develop and heat He<sup>+</sup> at the inner edge of the plasma sheet where a sufficient anisotropy develops in the energetic protons.

2. Low energy field aligned protons are observed simultaneously with the He<sup>+</sup> heating and might be contributing to the instability.

3. The heating appears to be modulated by a toroidal Pc 5.

[15] **Acknowledgments.** The work at the University of New Hampshire was supported by NASA under grant NAG5-6925. The Equator-S mission was supported via grand 500C94024 by the German Space Agency, DARA (now DLR).

## References

- Anderson, B. J., and S. A. Fuselier, Response of thermal ions to electromagnetic ion cyclotron waves, *J. Geophys. Res.*, *99*, 19,413–19,425, 1994.
- Anderson, B. J., M. J. Engebretson, S. P. Rounds, L. J. Zanetti, and T. A. Potemra, A statistical study of Pc 3–5 pulsations observed by the AMPTE/CCE magnetic field experiment. 1. Occurrence distributions, *J. Geophys. Res.*, *95*, 10,495–10,523, 1990.
- Anderson, B. J., R. E. Erlandson, and L. J. Zanetti, A statistical study of Pc 1–2 magnetic pulsations in the equatorial magnetosphere 1. Equatorial occurrence distributions, *J. Geophys. Res.*, *97*, 3075–3088, 1992a.
- Anderson, B. J., R. E. Erlandson, and L. J. Zanetti, A statistical study of Pc 1–2 magnetic pulsations in the equatorial magnetosphere 2. Wave properties, *J. Geophys. Res.*, *97*, 3089–3101, 1992b.
- Anderson, B. J., R. E. Denton, G. Ho, D. C. Hamilton, S. A. Fuselier, and R. J. Strangeway, Observational test of local cyclotron instability in the Earth's magnetosphere, *J. Geophys. Res.*, *101*, 21,527–21,543, 1996.
- Cornwall, J. M., Cyclotron instabilities and electromagnetic emission in the ultra low frequency and very low frequency ranges, *J. Geophys. Res.*, *70*, 61, 1965.
- Ejiri, M., R. A. Hoffman, and P. H. Smith, Energetic particle penetrations into the inner magnetosphere, *J. Geophys. Res.*, *85*, 6653–6663, 1980.
- Fornaçon, K. H., H. U. Auster, E. Georgescu, W. Baumjohann, K. H. Glasmeier, J. Rustenbach, and M. Dunlop, The magnetic field experiment onboard Equator-S and its scientific possibilities, *Ann. Geophysicae*, *17*, 1999.
- Fuselier, S. A., and B. J. Anderson, Low-energy He<sup>+</sup> and H<sup>+</sup> distributions and proton cyclotron waves in the afternoon equatorial magnetosphere, *J. Geophys. Res.*, *101*, 13,255–13,265, 1996.
- Gendrin, R., and A. Roux, Energization of helium ions by proton-induced hydromagnetic waves, *J. Geophys. Res.*, *85*, 4577–4586, 1980.
- Kennel, C. F., and H. E. Petschek, Limit on stably trapped particle fluxes, *J. Geophys. Res.*, *71*, 1–28, 1966.
- Mauk, B. H., C. E. McIlwain, and R. L. McPherron, Helium cyclotron resonance within the Earth's magnetosphere, *Geophys. Res. Lett.*, *8*, 103–106, 1981.
- Möbius, E., et al., The 3-D plasma distribution function analyzers with time-of-flight mass discrimination for CLUSTER, FAST, and Equator-S, in *Measurement Techniques in Space Plasmas: Particles*, edited by R. F. Pfaff, J. E. Borovsky, and D. T. Young, vol. 102, pp. 243–248, AGU, 1998.
- Nagai, T., J. F. E. Johnson, and C. R. Chappell, Low-energy (<100 eV) ion pitch angle distributions in the magnetosphere by ISEE 1, *J. Geophys. Res.*, *88*, 6944–6960, 1983.
- Rauch, J. L., and A. Roux, Ray tracing of ulf waves in a multicomponent magnetospheric plasma: Consequences for the generation mechanism of ion cyclotron waves, *J. Geophys. Res.*, *87*, 8191–8198, 1982.
- Rème, H., et al., The Cluster ion spectrometry experiment, *Space Sci. Rev.*, *79*, 303–350, 1997.
- Roux, A., S. Perraut, J. L. Rauch, C. de Villedary, G. Kremser, A. Korth, and D. T. Young, Wave-particle interactions near  $\Omega_{\text{He}^+}$  observed on board GEOS 1 and 2. 2. Generation of ion cyclotron waves and heating of He<sup>+</sup> ions, *J. Geophys. Res.*, *87*, 8174–8190, 1982.
- Young, D. T., S. Perraut, A. Roux, C. de Villedary, R. Gendrin, A. Korth, G. Kremser, and D. Jones, Wave-particle interactions near  $\omega_{\text{He}^+}$  observed on GEOS 1 and 2. 1. Propagation of ion cyclotron waves in He<sup>+</sup>-rich plasma, *J. Geophys. Res.*, *86*, 6755–6772, 1981.
- C. G. Mouikis, L. M. Kistler, E. J. Lund, E. Möbius, and M. A. Popecki, Space Science Center, Morse Hall, University of New Hampshire, Durham, NH, USA. (Chris.Mouikis@unh.edu)
- W. Baumjohann, Institut für Weltraumforschung, Graz, Austria.
- A. Korth, Max-Planck-Institut für Aeronomie, 37191 Katlenburg-Lindau, Germany.
- B. Klecker, Max-Planck-Institut für extraterrestrische Physik, Garching, Germany.
- J. A. Sauvaud and H. Rème, C.E.S.R., Toulouse, France.
- A. M. Di Lellis, I.F.S.I., Rome, Italy.
- M. McCarthy, University of Washington, Seattle, WA, USA.
- C. W. Carlson, University of California, Berkeley, CA, USA.